



ORIGINAL ARTICLE

Open Access



Control of system parameters by estimating screw withdrawal strength values of particleboards using artificial neural network-based statistical control charts

Rifat Kurt*

Abstract

In this study, with data obtained from a particleboard factory, screw withdrawal strength (SWS) values of particleboards were estimated using artificial neural networks (ANNs). Predictive control charts were also created. A total of seven independent variables were used for the ANN model: modulus of elasticity (MoE), surface soundness (SS), internal bond strength (IBS), density, press time, press temperature, and press pressure. The results showed that the ANN-based individual moving range (I-MR) and cumulative sum (CUSUM) control charts created for SWS values detected out-of-control signal points close to those of the real-time control charts. Among the selected independent variables, IBS was the most important parameter affecting SWS. The most suitable press temperatures and times for high SWS values were determined as 198–201 °C and 165–175 s, respectively. Moreover, the boards with 2500–2800 N/mm² MoE and 0.55 N/mm² IBS values exhibited the best SWS.

Keywords: Statistical process control, Artificial neural networks, Control charts, Particleboard

Introduction

In today's markets, strong competition is forcing businesses to seek more productive and economically effective undertakings. Meeting the ever-changing expectations and demands of customers is the main condition for the survival and development of a business. In this situation, because of the desire to obtain long-term market success, quality has become the main element in business strategy [1].

Businesses have increasingly begun to recognize that quality is a crucial factor in the success of their enterprises. The “total quality management” concept involves quality cost and its measurement [2]. Quality cost is the key factor necessary to put the total quality management philosophy into practice. Adopting quality cost

management can enable businesses to lower their costs without compromising the quality of their product or customer satisfaction [3, 4]. Strategic decision making based on quality cost will facilitate profit generation. Business status can be boosted by analyzing achievements and committing to improvements through the application of the quality cost account as part of efficient management [1].

Having full control of product efficiency and producing fewer faulty products are among the ways to reduce quality costs. Consequently, during the production process, industries use monitoring procedures that apply various technologies and methods to record the quality and properties of the product and to identify defective products. Quality control researchers often employ engineering process control (EPC) and statistical process control (SPC) techniques. These are useful applications for monitoring engineering processes and controlling them [5–8].

*Correspondence: rkurt@bartin.edu.tr

Department of Forest Industrial Engineering, Faculty of Forestry, Bartın University, Bartın, Turkey

The SPC is used to analyze information about sample products and to make decisions about processes. Such statistical approaches are crucial for quality assurance. This statistical method provides the main means of sampling, testing, and evaluating a product, and information from these data is utilized to control the manufacturing process and improve it [8, 9]. Thus, significant progress has been achieved in terms of revealing the deviations that may occur in quality characteristics and accordingly, in reducing production costs, increasing labor productivity, and protecting the consumer.

In the production process, the most important tools for understanding and interpreting the variability and chance of implementation are the control charts [10]. The main function of the SPC is to monitor the process for any early signs of external problems in the process via the use of control charts. Moreover, the SPC can propose possible joint measures to avoid the manufacture of any abnormal or defective products. A standard chart can also identify unstable conditions or aberrant variations that need to be investigated [5].

Under good quality management, warning signs would be provided in the early stages of a manufacturing project to facilitate timely interventions and to avoid limited options late in the process. Consequently, it is important to predict certain parameter values throughout various stages of the project with the aim of controlling these parameters during its implementation and thus ensuring that the desired quality is achieved in the final product [11].

Particleboards are produced from particles or chips of wood (or other lignocellulosic fibrous sources) held together by a binder and subjected to elevated pressure at a high temperature [12]. Particleboards have a smooth surface, can be produced in the desired thickness, have a relatively homogeneous structure, can be joined using nails, screws, and glues, can be produced in large sizes, and allow the application of top surface treatments [13]. These properties and important features of this composite product enable its extensive application in many usage areas.

Wood-based products (furniture, cabinets, tables, desks, etc.) made of particleboard are often subjected to significant loads, and thus threaded steel fasteners (screws) are used to join these products. The strength of these fasteners is at least 10 times higher than the strength of the wood-based materials. Because of overload on joinings made with steel screws, ruptures can occur in the wood-based board. Therefore, the bonding force is determined by the strength of the wood-based panel boards rather than by the screws [14, 15].

During the manufacturing process, the quality control measures applied are crucial for ensuring the production

of a quality final product that satisfies customer expectations. However, certain costs and expenditures of time are required for such processes [16].

The main purpose of this study was to predict different variables and screw withdrawal strength (SWR) values obtained from the particleboard production process without measuring, but rather by modeling via artificial neural networks (ANNs), and to create predictive control charts. Thus, the aim was to keep the production process under control with less measuring and to contribute to the reduction of the quality cost of businesses.

Previous studies have used different methods for estimating particleboard SWR [17–19] and for estimating different mechanical properties of particleboard [16, 20–24]. In addition, studies have also been carried out in different sectors on the estimation of different control charts [7, 25–28]. In this study, unlike other studies, in addition to estimating SWS values using ANNs, predictive control charts were also created. Thus, a model was developed that enables a business to receive early warning of errors. Moreover, to date, no studies on the particleboard industry have been conducted using ANNs to predict individual moving range (I-MR) and cumulative sum (CUSUM) control charts. The factors effective on SWS were also determined and the relationships between them were revealed in detail in this study.

Preliminaries

Artificial neural networks

ANNs are mechanisms for processing information that are based on the biological processes of the nervous system. Like the nervous system, ANNs are composed of a great number of interconnected, and in this case artificial, neurons acting as processing elements working together to solve specific problems [29]. Thus, the ANN is a mathematical model attempting to simulate biological neuron behavior [30]. A neuron can generate an output signal on the basis of a specific number of input signals. The activation function processes input signals generated by other neurons. To generate an output signal, the activation function value is transmitted to the transfer function. A neural network is composed of three layers: the input layer, the output layer, and the hidden layer. Data from outside the ANN are received by the neurons of its input layer, whereas data processing results are presented by the neurons of the output layer [31]. Equation (1) describes the function of the network [16, 32]:

$$Y_j = f\left(\sum_i w_{ij}x_{ij}\right) \quad (1)$$

where Y_j represents the node j output, f represents the transfer function, W_{ij} represents the weight connecting

node j and node i in the lower layer, and X_{ij} represents the input signal from node i in the lower layer node j .

The three main phases necessary to set up an ANN include: (1) establishment of the ANN architecture, (2) definition of the appropriate training algorithm necessary for the ANN learning phase, and (3) determination of the mathematical functions describing the mathematical model [30]. The ANN is used in many areas such as classification, modelling, data association—interpretation, control, clustering, and optimization [33, 34]. When applied to a network, the learning algorithm and its structure will determine the learning performance. The classification ability and prediction quality of the network depend on application of a learning algorithm based on synaptic weights between the neurons.

I-MR control chart

I-MR charts can monitor individual values and detect any variations in the process over time by taking process samples over hours, shifts, days, weeks, months, etc. [35]. These I-MR control charts were chosen for the study, because the values estimated by the ANN were the averages of the SWS values, and therefore, it was not possible to create a range of variation (R) graph for the estimated control charts. A moving range (MR) graph was constructed by plotting the Upper Control Limit (UCL), Lower Control Limit (LCL), and Center Line (CL) as given in Eq. (2) [8, 36]:

$$\begin{aligned} \text{UCL} &= D_4 \overline{MR} \\ \text{CL} &= \overline{MR} \\ \text{LCL} &= D_3 \overline{MR} \end{aligned} \quad (2)$$

where \overline{MR} is the average of the moving range computed from a preliminary set of data.

The MR was calculated using the following equation:

$$MR_i = |x_i - x_{i-1}|, i = 2, 3, \dots \quad (3)$$

Finally, the individual (I) chart was set up by plotting the individual observations, x_i , on a chart with limits, as in Eq. (4):

$$\begin{aligned} \text{UCL} &= \bar{x} + 3 \frac{\overline{MR}}{d_2} \\ \text{CL} &= \bar{x} \\ \text{LCL} &= \bar{x} - 3 \frac{\overline{MR}}{d_2} \end{aligned} \quad (4)$$

where D_3 , D_4 , and d_2 are functions of the sample size. According to the sample size, tables were created for these values.

CUSUM control chart

In 1954, Page [37] the CUSUM control chart, which consists of a series of consecutive operations used to detect any deviations in a process. The CUSUM control scheme is based on probability ratios and its principal feature is its ability to calculate the difference between an observed value and a predetermined target value [38]. The cumulative sum is determined using \bar{x}_j as the average of the j th sample and μ_0 as the target for the process mean; C_i denotes the cumulative sum up to and including the i th sample:

$$C_i = \sum_{j=1}^i (\bar{x}_j - \mu_0) \quad (5)$$

The tabular CUSUM statistic is used to detect an increase (C_i^+) or decrease (C_i^-) in the process mean shift:

$$C_i^+ = \max[0, x_i - (\mu_0 + K) + C_{i-1}^+] \quad (6)$$

$$C_i^- = \min[0, x_i - (\mu_0 - K) + C_{i-1}^-]$$

where μ_0 is the acceptable process mean.

The K value (i.e., the reference/allowance/slack value) is often set to half the distance between the target μ_0 and the out-of-control value of the mean μ_1 , for which a rapid detection is sought in Eq. (7):

$$K = \frac{\delta}{2} \sigma = \frac{|\mu_1 - \mu_0|}{2} \quad (7)$$

The process is said to be out of control if

$$C_i \geq H \quad (8)$$

where H is the decision interval. It is also customary to take $K=0.5$ and $H=4$ or 5 as decision parameters for the optimum average run length (ARL) [8, 39, 40].

Minor changes in the process average can be quite effectively detected by the CUSUM control charts [41, 42]. These charts have the advantage of being able to detect unstable processes for data subgroups and single notations [43].

Materials and methods

The data used in the study were obtained between February and July 2016 from a large-scale furniture enterprise operating in Turkey. The boards from which the

samples were taken were 18 mm thick, with a density of 630 kg/m^3 and were $2100 \times 2800 \text{ mm}$ in size. They were produced for interior hardware applications in dry conditions determined according to TS EN 310, TS EN 311, TS EN 319, and TS EN 320 standards [44–47]. In the said period, each particleboard from the production process was evaluated in terms of the screw withdrawal strength (SWS, N), modulus of elasticity (MoE, N/mm^2), surface soundness (SS, N/mm^2), internal bond strength (IBS, N/mm^2), and density (Kg/m^3) values and values related to press conditions, including press time (s), press temperature ($^{\circ}\text{C}$), press pressure (Pa), were measured. The sample size (n) was 3 and the number of samples (m) was 110, i.e., $110 \times 3 = 330$ measurements taken for each variable. From these data, 80 were used in the creation of the ANN model (training, testing, and validation), and the remaining 30 were used in the verification of the established model and in the creation of control charts to measure its success.

Our ANN model consisted of the input layer that receives the data from the outside, the output layer that yields the outputs of the network, and the multilayer perceptron, which consists of at least one hidden layer between the other two. Multilayer perceptrons are commonly used in the literature. These are feed-forward supervised networks with full connectivity between the layers [48–50]. The ANN model used in the study was designed as a feedforward back propagation model and is presented in Fig. 1.

In the figure, the input layer consists of the MoE, SS, tensile strength, density, press time, press temperature, and press pressure values as the independent variables to be used for estimation. These determined variables also form the number of neurons in the input layer of the ANN model. The number of hidden layers in the model was 1. There is no fixed rule for determining the number of neurons in the hidden layer. In general, keeping the number of hidden neurons low can cause learning problems in the network, whereas keeping it high can cause the network to memorize instead of learning. For

this reason, trials were carried out for 1–10 hidden neurons to determine the best number for the model and the result was found to be 8. The output neuron was directly related to the problem under study, and therefore, it was considered as being equal to the number of dependent variables estimated in the prediction problems. Thus, the output neuron here was the SWS. The sigmoid activation function is the one most commonly used in ANNs, and therefore, it was chosen as the activation function. Of the data in the model, 70% were used for training, 15% for validation, and 15% for testing. During the training phase of the network, the number of cycles was kept constant at 1000 and as a result of different trials, the most appropriate learning coefficient was determined as 0.1 and the momentum coefficient as 0.8. After the training and testing stages of the model were carried out successfully, 30 average SWS values were estimated using the established model. Separate I-MR and CUSUM control charts were created for these prediction and real-time measurement values, and the prediction performance of the model was evaluated. In the last part of the study, the statistical effect of the selected independent variables on the SWS values was investigated and analyzed in detail. MATLAB (MathWorks Inc.) software was used to establish the ANN model, and MINITAB software was used for quality control charts and statistical analyses.

Results

Establishment of the ANN: training, testing, and validation

Figure 2 shows the variation in the error values of the training, validation, and test sets in each iteration of the ANN model established for the estimation of the SWS values. Graphs showing the status of the training and the regression values are also presented. The regression values obtained for the training, validation, and testing stages were more than 80% and thus within the limits that can be used for estimation.

The established model was assessed in terms of the success of its predictive ability using never-before-seen data to test the network, and this approach yielded

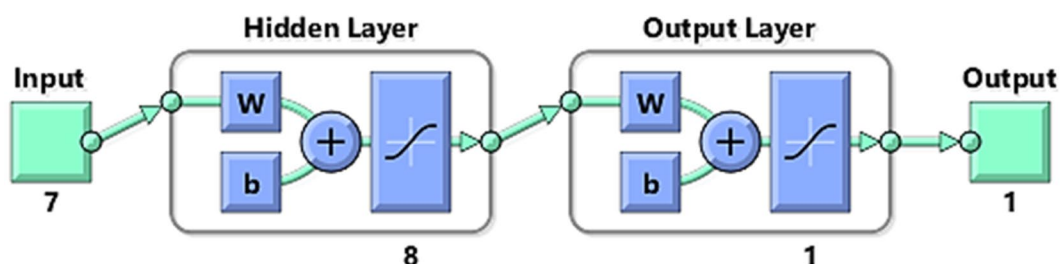


Fig. 1 Structure of the ANN model

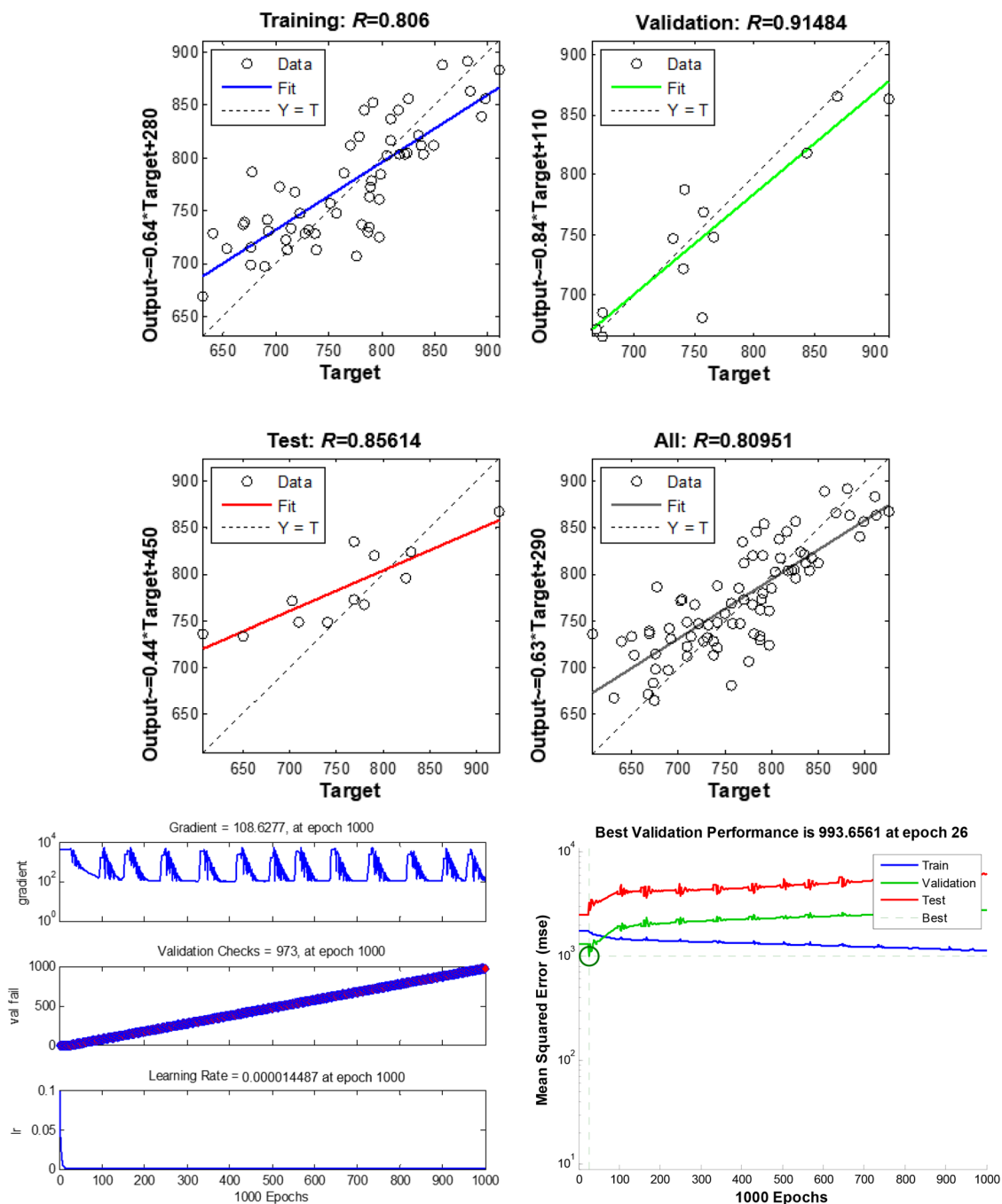


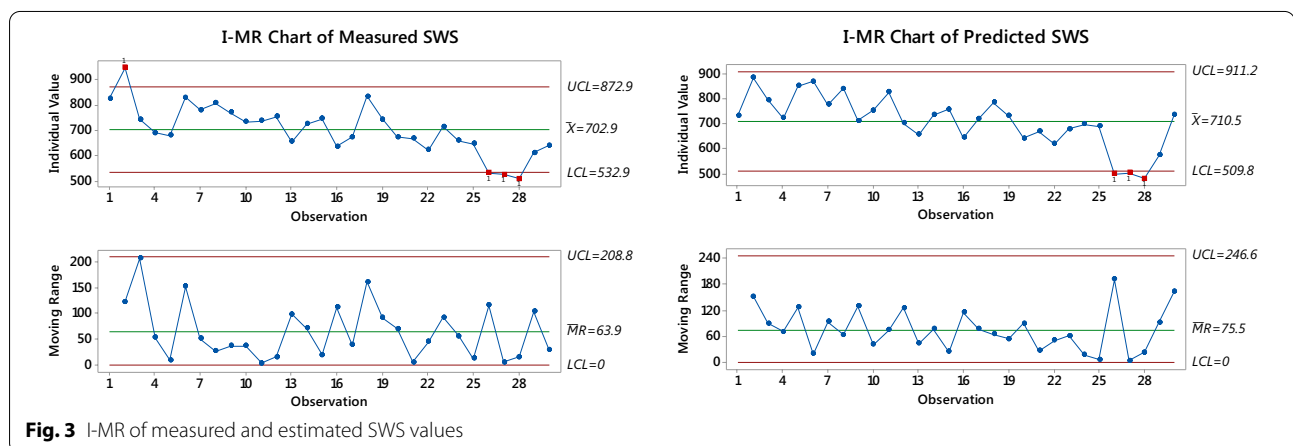
Fig. 2 ANN training, validation, and test results

positive results. A comparison of the estimated ANN values with the measured SWS values and their mean absolute percentage error (MAPE) performance values are given in Table 1. According to the MAPE values, the estimation process had been quite successful. In

the literature, models with MAPE values below 10% are rated “very good”, 10–20% “good”, 20–50% “acceptable”, and models over 50% “wrong and erroneous” [51–53]. The mean MAPE value of all predicted values was 5.79%.

Table 1 SWS estimated, measured, and MAPE values

Sample no	Measured	Estimated	MAPE	Sample no	Measured	Estimated	MAPE
1	825.0	733.7	11.1	16	634.7	644.1	1.5
2	947.3	886.4	6.4	17	673.7	721.8	7.1
3	742.0	796.0	7.3	18	833.3	787.2	5.5
4	689.3	724.8	5.1	19	742.3	732.5	1.3
5	679.3	852.1	25.4	20	672.3	641.8	4.5
6	830.0	872.3	5.1	21	666.0	669.8	0.6
7	779.3	778.3	0.1	22	621.0	619.0	0.3
8	806.7	842.7	4.5	23	713.3	680.5	4.6
9	770.0	712.5	7.5	24	657.7	698.2	6.2
10	732.7	754.1	2.9	25	645.0	690.9	7.1
11	736.7	828.6	12.5	26	530.3	498.9	5.9
12	752.3	702.0	6.7	27	524.0	504.0	3.8
13	654.3	657.4	0.5	28	507.7	480.1	5.4
14	725.3	735.4	1.4	29	611.0	573.3	6.2
15	745.3	760.0	2.0	30	640.0	737.3	15.2

**Fig. 3** I-MR of measured and estimated SWS values

Creation of control charts

Figure 3 shows the I-MR charts created for the measured and estimated SWS values. When the graphs are compared, the points that give out-of-control signals in the production process are shown as almost the same in both graphs. Sample nos. 26, 27, and 28 on both charts are outside the LCL. However, one point in the measurement values (sample no. 2) exceeded the UCL, and the I-MR graph created via estimation was unable to detect this. However, sample no. 2 in the estimation chart was very close to the UCL limit, but because a high SWS is desirable, this situation did not last for long.

In Fig. 4, the measured and estimated SWS values for the CUSUM control charts are given. The CUSUM charts are particularly effective at detecting minor shifts in the

process. Both graphs were very close in clearly determining the shifts in the process. In particular, the estimated (predicted) CUSUM graph detected the negative shift after sample no. 26 in the same way as did the real (measured) CUSUM graph.

Correlation analysis

This section gives the results of the investigation into the effect of the selected independent variables on the SWS. Table 2 shows that in general, all variables except the SS exhibited a significant positive correlation with the SWS at 1% and 5% significance levels. The IBS was the most important parameter affecting the SWS. In the literature, correlation values with an r coefficient of 0.40–0.59 are defined as “moderate” [54–58]. Figure 5 presents

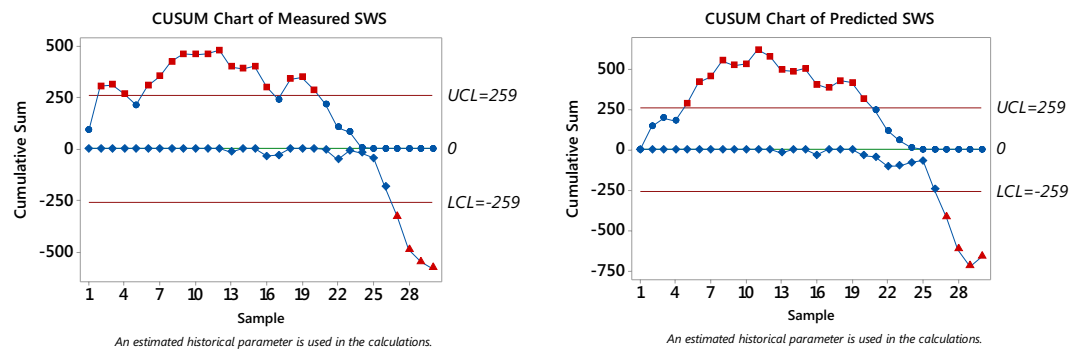


Fig. 4 CUSUM charts of measured and estimated SWS values

Table 2 Pearson correlation results

Correlations	Pearson correlation (SWS)	Significance level	Significance (two-tailed)
Internal bond strength (IBS)	0.659	0.01	0.000
Press temperature	0.539	0.01	0.000
Press time	0.530	0.01	0.000
Modulus of elasticity (MoE)	0.426	0.01	0.000
Press pressure	0.360	0.01	0.001
Density	0.204	0.05	0.032
Surface soundness (SS)	0.055	–	0.569

surface plots and contour plots showing the relationships between moderately significant parameters and SWS values.

The temperature–time graph of SWS values shows generally, the SWS of the particleboards also increased with the increase in press temperature and press time (Fig. 5). Again, in the contour plot, the highest SWS value was reached at press temperatures of 198–201 °C and at press times in the range of 165–175 s. In previous studies, increases in press temperature [59–62] and press time [60, 63, 64] have been reported to affect SWS positively. Examination of the MoE-IBS graphs of the SWS shows that the high IBS and MoE values had a positive effect on SWS. In the literature, similar associations have been found between IBS and SWS [19, 21, 65–73] and between SWS and MoE [65, 66, 68–70, 73, 74]. In the counter graph, the boards with MoE values of 2500–2800 N/mm² and an IBS value of 0.55 N/mm² have the highest SWS values.

Conclusion and recommendations

In this study, particleboard SWS values were estimated in a production process via modeling using an ANN. Statistical control charts were created with these estimated values and compared with the real-time production values. For the established ANN model, the most appropriate learning coefficient was determined as 0.1, the momentum coefficient as 0.8, and the number of neurons in the hidden layer as 8. A regression value of over 80% was obtained in the training, validation, and testing stages of the particleboard SWS values estimated using seven independent variables in the input layer. The MAPE values of the measured and estimated SWS values were within the limits accepted as “very good” in the literature, with an average of 5.79%. The control charts created with these estimates yielded results very similar to those in the control charts created with the real values. The predicted CUSUM and I-MR control charts detected the values that exceeded the LCL, which is very important for a business. In addition, among the independent variables selected in the Pearson correlation analysis, the most important parameter affecting the SWS was determined as IBS, with a correlation of 0.69. The most suitable press temperatures and times for high SWS values were determined as 198–201 °C and 165–175 s, respectively. In addition, the boards with 2500–2800 N/mm² MoE and 0.55 N/mm² IBS values exhibited the best SWS values.

Numerous parameters affect the mechanical properties of particleboard. In future studies, new models could be developed using different parameters such as chip mixing ratios, glue type and amount, or based on wood species. Control charts could be created by estimating different technological and mechanical properties of the board, thus contributing to the reduction of quality costs for businesses.

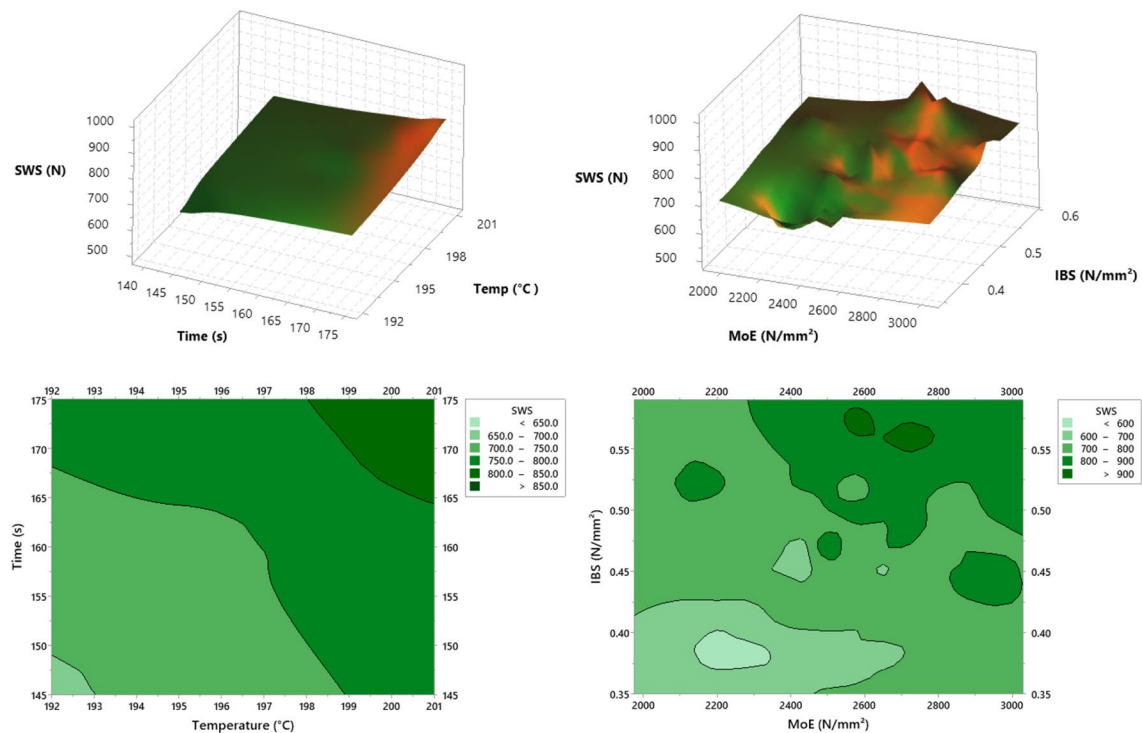


Fig. 5 Surface plot and contour plots of parameters affecting SWS values. Green colors: SWS values, Orange colors: points where SWS tends to increase

Abbreviations

SWS: Screw withdrawal strength; ANN: Artificial neural network; MoE: Modulus of elasticity; SS: Surface soundness; IBS: Internal bond strength; I-MR: Individual moving range; CUSUM: Cumulative sum; EPC: Engineering process control; SPC: Statistical process control; R: Range of variation; MR: Moving range; UCL: Upper control limit; LCL: Lower control limit; CL: Center line; I: Individual; ARL: Average run length; MAPE: Mean absolute percentage error.

Acknowledgements

Not applicable.

Author contributions

RK designed and conducted the study, analyzed the data, and wrote the manuscript. The author read and approved the final manuscript.

Funding

No funding.

Availability of data and materials

The data that support the findings of this study are available from the corresponding author, Rifat Kurt.

Declarations

Competing interests

The author declares that he has no known competing financial interests or personal relationships that could appear to have influenced the work reported in this paper.

Received: 10 June 2022 Accepted: 6 November 2022

Published online: 08 December 2022

References

1. Tkaczyk S, Jagla J (2001) Economic aspects of the implementation of a quality system process in polish enterprises. *J Mater Process Technol* 109:196–205. [https://doi.org/10.1016/S0924-0136\(00\)00796-2](https://doi.org/10.1016/S0924-0136(00)00796-2)
2. Kendirli S, Tuna M (2009) Quality cost's constitution and effects on financial decision in enterprises: a research in Corum's enterprises. *Proceedings of the Academy of Accounting and Financial Studies* 14:21–32
3. Murumkar A, Teli SN, Loni RR (2018) Framework for reduction of quality cost. *international journal of research in engineering application & management* 156–162
4. Maslak O, Grishko N, Maslak M, Skliar M (2020) Quality costs of machine-building enterprises in Ukraine: a control mechanism. *Technium Soc Sci J* 9:326–336. <https://doi.org/10.47577/tssj.v9i1.1163>
5. Al-Ghanim A, Jordan J (1996) Automated process monitoring using statistical pattern recognition techniques on x-bar control charts. *J Qual Maint Eng* 2:25–49. <https://doi.org/10.1108/13552519610113827>
6. Wu Z, Shamsuzzaman M (2005) Design and application of integrated control charts for monitoring process mean and variance. *J Manuf Syst* 24:302–314. [https://doi.org/10.1016/S0278-6125\(05\)80015-9](https://doi.org/10.1016/S0278-6125(05)80015-9)
7. Kao LJ, Chiu CC (2020) Application of integrated recurrent neural network with multivariate adaptive regression splines on SPC-EPC process. *J Manuf Syst* 57:109–118. <https://doi.org/10.1016/j.jmsy.2020.07.020>
8. Montgomery DC (2019) *Introduction to statistical quality control*, 8th edn. Wiley, Hoboken
9. Andalia W, Pratiwi I, Arita S (2019) Analysis of biodiesel conversion on raw material variation using statistical process control method. *J Phys Conf Ser* 1167:1–7
10. Ozdamar IH (2007) Statistical process control in forest products industry: case study on particleboard production process. *Turkish J For* 8:79–91
11. Jalote P, Dinesh K, Raghavan S, Bhashyam MR, Ramakrishnan M (2000) *Quantitative quality management through defect prediction and statistical process control*^T. Electronics, Basel.
12. EN 309 (2005) *Particleboards: definition and classification*. European standard.

13. Istek A, Gozalan M, Ozluosoylu I (2017) The effects of surface coating and painting process on particleboard properties. *Kastamonu Univ J For Fac* 17:619–629. <https://doi.org/10.17475/kastorman.180279>
14. Sahin HI, Yalcin M, Yaglica N (2017) Determination of screw holding and thermal conductivity values of core layer compost waste additive particleboard. *Artvin Coruh Univ J For Fac* 18:121–129. <https://doi.org/10.17474/artvinofd.320521>
15. Smardzewski J, Klos R (2011) Modeling of joint substitutive rigidity of board elements. *annals of Warsaw University of life science—SGGW. For Wood Technol* 73:7–15
16. Kurt R, Karayilmazlar S (2019) Estimating modulus of elasticity (MOE) of particleboards using artificial neural networks to reduce quality measurements and costs. *Drvna Industrija* 70:257–263. <https://doi.org/10.5552/drvid.2019.1840>
17. Arabi M, Faezipour M, Haftkhani AR, Maleki S (2012) The effect of particle size on the prediction accuracy of screw withdrawal resistance (SWR) models. *J Indian Acad Wood Sci* 9:53–56. <https://doi.org/10.1007/s13196-012-0063-6>
18. Bobadilla I, Arriaga F, Esteban M, Iñiguez G, Blázquez I (2008) Density estimation by vibration, screw withdrawal resistance and probing in particle and medium density fibre boards. 10th world conference on timber engineering. 3:1423–1430
19. Semple KE, Smith GD (2006) Prediction of internal bond strength in particleboard from screw withdrawal resistance models. *Wood Fiber Sci* 38:256–267
20. Bardak S (2018) Predicting the impacts of various factors on failure load of screw joints for particleboard using artificial neural networks. *BioResources* 13:3868–3879. <https://doi.org/10.15376/biores.13.2.3868-3879>
21. Haftkhani AR, Arabi M (2013) Improve regression-based models for prediction of internal-bond strength of particleboard using Buckingham's pi-theorem. *J For Res* 24:735–740. <https://doi.org/10.1007/s11676-013-0412-3>
22. Tas HH, Cetisli B (2016) Estimation of physical and mechanical properties of composite board via adaptive neural networks, polynomial curve fitting, and the adaptive neuro-fuzzy inference system. *BioResources* 11:2334–2348. <https://doi.org/10.15376/biores.11.1.2334-2348>
23. Korai H (2021) Difficulty of internal bond prediction of particleboard using the density profile. *J Wood Sci* 67:1–7. <https://doi.org/10.1186/s10086-021-01994-4>
24. Zhang B, Hua J, Cai L, Gao Y, Li Y (2022) Optimization of production parameters of particle gluing on internal bonding strength of particleboards using machine learning technology. *J Wood Sci* 68:1–11. <https://doi.org/10.1186/s10086-022-02029-2>
25. Arabgol S, Ko HS, Esmaili S (2015) Artificial neural network and EWMA-based fault prediction in wind turbines. *IIE annual conference and expo* 2015:829–836
26. Fehlmann T, Kranich E (2014) Exponentially weighted moving average (EWMA) prediction in the software development process. 2014 Joint Conference of the international workshop on software measurement and the international conference on software process and product measurement 2014:263–270. <https://doi.org/10.1109/IWSM.Mensura.2014.50>
27. Alwan LC, Roberts HV (1989) Time-series modeling for statistical process control. *J Bus Econ Stat* 6:87–95. <https://doi.org/10.1080/07350015.1988.10509640>
28. Wang XA, Mahajan RL (1996) Artificial neural network model-based run-to-run process controller. *IEEE Trans Compon Packag Manuf Technol Part C* 19:19–26. <https://doi.org/10.1109/3476.484201>
29. Kucukoglu I, Atici-Ulus H, Gunduz T, Tokcalar O (2018) Application of the artificial neural network method to detect defective assembling processes by using a wearable technology. *J Manuf Syst* 49:163–171. <https://doi.org/10.1016/j.jmsys.2018.10.001>
30. Asteris PG, Mokos VG (2020) Concrete compressive strength using artificial neural networks. *Neural Comput Appl* 32:11807–11826. <https://doi.org/10.1007/s00521-019-04663-2>
31. Iannace G, Ciaburro G, Trematerra A (2020) Modelling sound absorption properties of broom fibers using artificial neural networks. *Appl Acoust* 163:1–9. <https://doi.org/10.1016/j.apacoust.2020.107239>
32. Kurt R (2019) Determination of the most appropriate statistical method for estimating the production values of medium density fiberboard. *BioResources* 14:6186–6202. <https://doi.org/10.15376/biores.14.3.6186-6202>
33. Kurt R, Karayilmazlar S, Imren E, Cabuk Y (2017) Forecasting by using artificial neural networks: Turkey's paper-paperboard industry case. *J Bartin Fac For* 19:99–106. <https://doi.org/10.24011/barofd.334773>
34. Imren E, Kaygin B, Karayilmazlar S (2021) Evaluation of foreign trade data of Turkish furniture industry with artificial neural networks. *J Bartin Fac For* 23:906–916. <https://doi.org/10.24011/barofd.1011207>
35. NCSS statistical software (2022) Individuals and moving range charts. <https://www.ncss.com/software/ncss/quality-control-in-ncss/>. Accessed 21 April 2022
36. Khoo MBC, Quah SH, Ch'ng CK, (2006) A combined individuals and moving range control chart. *J Mod Appl Stat Method* 5:248–257. <https://doi.org/10.22237/jmasm/1146457140>
37. Page ES (1954) Continuous inspection schemes. *Biometrika* 41:100–115. <https://doi.org/10.2307/2333009>
38. Adeoti OA (2013) Application of Cusum control chart for monitoring HIV/AIDS patients in Nigeria. *Int J Stat Appl* 3:77–80. <https://doi.org/10.5923/j.statistics.20130303.07>
39. Hawkins DM, Olwell DH (1998) Cumulative sum charts and charting for quality improvement. Springer, Berlin. <https://doi.org/10.1007/978-1-4612-1686-5>
40. Ikpotokin O, Braimah JO, Oboh HE (2021) Performance evaluation of conventional exponentially weighted moving average (EWMA) and p-value cumulative sum (CUSUM) control chart. *Global J Pure Appl Sci* 27:171–179. <https://doi.org/10.4314/gjpas.v27i2.9>
41. Kurt R, Karayilmazlar S (2021) Which control chart is the best for particleboard industry: Shewhart, CUSUM or EWMA? *Drewno* 64:95–117. <https://doi.org/10.12841/wood.1644-3985.382.07>
42. Aslam M, Shafqat A, Albassam M, Malela-Majika J, Shongwe SC (2021) A new CUSUM control chart under uncertainty with applications in petroleum and meteorology. *PLoS ONE* 16:1–16. <https://doi.org/10.1371/journal.pone.0246185>
43. Sunthornwat R, Areepong Y (2020) Average run length on CUSUM control chart for seasonal and non-seasonal moving average processes with exogenous variables. *Symmetry* 12:1–15. <https://doi.org/10.3390/SYM12010173>
44. En TS (2005) 311, Wood-based panels, surface soundness, test method. Turkish Standards Institution, Ankara
45. En TS (1999) 319, Particleboards and fibreboards, determination of tensile strength perpendicular to the plane of the board. Turkish standards institution, Ankara
46. En TS (1999) 310, Wood-Based panels, determination of modulus of elasticity in bending and of bending strength. Turkish standards institution, Ankara
47. En TS (2011) 320 Particleboards and fibreboards, determination of resistance to axial withdrawal of screws. Turkish standards institution, Ankara
48. Haykin S (1999) Neural networks: a comprehensive foundation, 3rd edn. Prentice Hall, Hoboken
49. Beale MH, Hagan MT, Demuth HB (2010) Neural network Toolbox™ user's guide MATLAB. MathWorks 2:77–81
50. Kurt R (2018) Integrated use of artificial neural networks and Shewhart, CUSUM and EWMA control charts in statistical process control: a case study in forest industry enterprise. Bartin University, Bartin, 209
51. Lewis CD (1997) Demand forecasting and inventory control. Routledge, London
52. Wang CC, Wang HY, Chen BT, Peng YC (2017) Study on the engineering properties and prediction models of an alkali-activated mortar material containing recycled waste glass. *Constr Build Mater* 132:130–141. <https://doi.org/10.1016/j.conbuildmat.2016.11.103>
53. Syafwan H, Syafwan M, Syafwan E, Hadi AF, Putri P (2021) Forecasting unemployment in North Sumatra using double exponential smoothing method. *J Phys Conf Ser* 1783:1–6. <https://doi.org/10.1088/1742-6596/1783/1/012008>
54. Evans JD (1996) Straightforward statistics for the behavioral sciences. Brooks/Cole, Pacific Grove
55. Wuensch KL (1996) Straightforward statistics for the behavioral sciences by James D. Evans. *J Am Stat Assoc* 91:1750–1751. <https://doi.org/10.2307/2291607>
56. Toneva D, Nikolova S, Georgiev I, Harizanov S, Zlatareva D, Hadjidekov V, Lazarov N (2018) Facial soft tissue thicknesses in Bulgarian adults: relation to sex, body mass index and bilateral asymmetry. *Folia Morphol* 77:570–582. <https://doi.org/10.5603/FM.a2017.0114>

57. Rathnayaka IMSK, Dharmapriya TN, Liyandeniya AB, Deeyamulla MP, Priyantha N (2020) Trace metal composition of bulk precipitation in selected locations of Kandy district, Sri Lanka. *Water Air Soil Pollut* 231:1–12. <https://doi.org/10.1007/s11270-020-04840-3>
58. Campbell MJ (2021) *Statistics at square one*, 12th edn. Wiley, Hoboken
59. Ferrández-García CE, Andréu-Rodríguez FJ, Ferrández-García MT, Ferrández-Villena M, García-Ortuño T (2010) Effect of press temperature on physical and mechanical properties of particleboard made from giant reed (*Arundo donax* L.). In *International Conference on Agricultural Engineering-AgEng 2010: Towards Environmental Technologies*, France. 6–8
60. Warmbier K, Wilczyński M, Danecki L (2014) Effects of some manufacturing parameters on mechanical properties of particleboards with the core layer made from willow *salix viminalis*. *Annals Warsaw Univ Life Sci SGGW For Wood Technol* 88:277–281
61. Korkmaz M, Kilinc I, Yapici F, Baydag M (2017) The investigation of the effects of production factors on the screw holding resistance value of oriented strand board (OSB). *J Adv Technol Sci* 6:940–948
62. Widyorini R (2020) Evaluation of physical and mechanical properties of particleboard made from petung bamboo using sucrose-based adhesive. *BioResources* 15:5072–5086. <https://doi.org/10.15376/biores.15.3.5072-5086>
63. Kumas I (2013) Production of different conditions on the technological properties of particleboard manufactured from alder (*Alnus glutinosa* subsp. *Barbata*). Karadeniz Technical University, Trabzon, 85
64. Camlibel O (2021) The effect of multi-layers hot press on mechanical properties of particleboard. *Turkish J Agric Nat Sci* 8:800–807. <https://doi.org/10.30910/turkjans.870258>
65. Kalaycioglu H, Deniz I, Hizioglu S (2005) Some of the properties of particleboard made from paulownia. *J Wood Sci* 51:410–414. <https://doi.org/10.1007/s10086-004-0665-8>
66. Nemli G, Ors Y, Kalaycioglu H (2005) The choosing of suitable decorative surface coating material types for interior end use applications of particleboard. *Constr Build Mater* 19:307–312. <https://doi.org/10.1016/j.conbuildmat.2004.07.015>
67. Sackey EK, Semple KE, Oh SW, Smith GD (2008) Improving core bond strength of particleboard through particle size redistribution. *Wood Fiber Sci* 40:214–224
68. Lin CJ, Hizioglu S, Kan SM, Lai HW (2008) Manufacturing particleboard panels from betel palm (*Areca catechu* Linn.). *J Mater Process Technol* 197:445–448. <https://doi.org/10.1016/j.jmatprotec.2007.06.048>
69. Guruler H, Balli S, Yeniocak M, Goktas O (2015) Estimation the properties of particleboards manufactured from vine prunings stalks using artificial neural networks. *Mugla J Sci Technol* 1:24–33. <https://doi.org/10.22531/muglajsci.209996>
70. Waelaeh S, Tanrattanakul V, Phunyarat K, Panupakorn P, Junnam K (2017) Effect of polyethylene on the physical and mechanical properties of particleboard. *Macromol Symp* 371:8–15. <https://doi.org/10.1002/masy.201600030>
71. Ab Hafidz MY, Mohd AF, Zulkifli M (2018) Mechanical properties and formaldehyde emission of rubberwood particleboard using emulsified methylene diphenyl diisocyanate (EMDI) Binder at different press factor continuous press. *Int J Eng Technol* 7:335–338. <https://doi.org/10.14419/ijet.v7i4.14.27669>
72. Chung MJ, Wang SY (2019) Physical and mechanical properties of composites made from bamboo and woody wastes in Taiwan. *J Wood Sci* 65:1–10. <https://doi.org/10.1186/s10086-019-1833-1>
73. Choupani Chaydarreh K, Lin X, Guan L, Hu C (2022) Interaction between particle size and mixing ratio on porosity and properties of tea oil camellia (*Camellia oleifera* Abel.) shells-based particleboard. *J Wood Sci* 68:1–12. <https://doi.org/10.1186/s10086-022-02052-3>
74. Sampathrajan A, Vijayaraghavan NC, Swaminathan KR (1992) Mechanical and thermal properties of particle boards made from farm residues. *Biores Technol* 40:249–251. [https://doi.org/10.1016/0960-8524\(92\)90151-M](https://doi.org/10.1016/0960-8524(92)90151-M)

Publisher's Note

Springer Nature remains neutral with regard to jurisdictional claims in published maps and institutional affiliations.

Submit your manuscript to a SpringerOpen[®] journal and benefit from:

- Convenient online submission
- Rigorous peer review
- Open access: articles freely available online
- High visibility within the field
- Retaining the copyright to your article

Submit your next manuscript at ► [springeropen.com](https://www.springeropen.com)